Optica Applicata, Vol. XLII, No. 1, 2012
DOI: 10.5277/oa120110

A 2-bit polymer waveguide delay device using right-angle X junctions

YUNJI YI, QI WANG, PENGCHENG ZHAO, FEI WANG*, DAMING ZHANG

State Key Laboratory on Integrated Optoelectronics, Jilin University Region, Qianjin Street 2699, Changchun 130012, China

*Corresponding author: wang_fei@mail.jlu.edu.cn

A 2-bit polymer waveguide delay device composed of right-angle junctions, Mach–Zehnder thermo-optic switches and bending polymer waveguides is demonstrated. The four path device and Mach–Zehnder thermo-optic switch are fabricated using direct ultraviolet photolithography process. The fabrication procedures are demonstrated. The loss of bending waveguides, right-angle X junctions and Mach–Zehnder thermo-optic switches is calculated and analyzed. The near-infrared field guided-mode patterns of the device are obtained. Time delays of the 2-bit device are measured to be 0, 121.1, 242.3, and 365.7 ps.

Keywords: optical true time delay (OTTD), phased array radar, photonic integrated circuit (PIC), waveguide junctions.

1. Introduction

Optical true time delay (OTTD) technology is a promising technology in ultra-wide bandwidth phased array antenna (PAA) systems. With this technology, the beam squint effect can be eliminated, for the beam-steering direction of the phased array antennas is determined only by the time delay between the different optical elements. Because the RF signals are transmitted via the optical fiber or the waveguide, the noise due to the external electromagnetic interference can be greatly reduced. Several OTTD technologies have been proposed and demonstrated, including acousto-optic (AO) integrated circuit technique [1–3], Fourier optical technique [4–6], bulky optics techniques [7–12], slow light approach [13, 14], and substrate guided wave techniques [15–17]. A great deal of materials have been used to fabricate OTTD devices [18–21]. Polymer is considered as promising material, which has adjustable refractive indices, generally higher thermo-optic coefficients and lower thermal conductivities. Polymer can be coated on most of the substrates, which can reduce manufacturing costs and open the possibility of integrating a single chip with active PAA components.

An OTTD is typically composed of a series of optical delay lines with different optical paths, and a set of optical switches to select optical paths for a specific time

delay. A 2-bit polymer OTTD device with delays up to 199.2 ps has been reported with an insertion loss 9.81 dB [19]. In this paper, we report a 2-bit OTTD device with delays up to 366 ps. In order to achieve a large time delay between adjacent waveguides in finite space, a cross spiral waveguide array is introduced. Four Mach–Zehnder (MZ) thermo-optic switches were involved in the design. SU-8, a negative tone photoresist from MicroChem, is selected to be the channel waveguide core material. The upper and under cladding layers are made of a UV-cured resin, Norland Optical Adhesive 61 (NOA-61). The refractive indices of the core, lower cladding and upper cladding materials are 1.571, 1.547 and 1.547, respectively.

2. Design, fabrication, experiment result

Figure 1 shows the design of the OTTD device. Figure 1**a** shows schematic of a 1×4 OTTD device in a rectangular chip with dimensions of 1.5 cm×1.8 cm. Numbers 1 and 4 stand for the input and output numbers. The 1×4 OTTD contains a 1×4 splitter. The spacing between the output waveguide array of the splitter is 40 μm. The angle

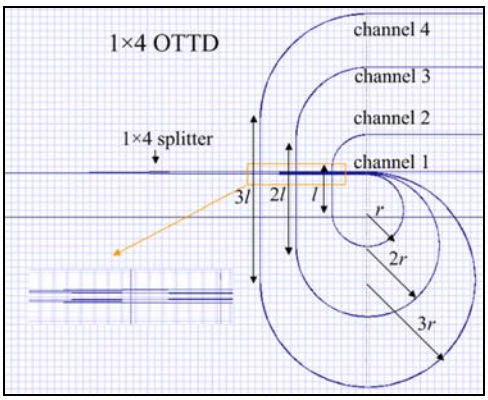

a

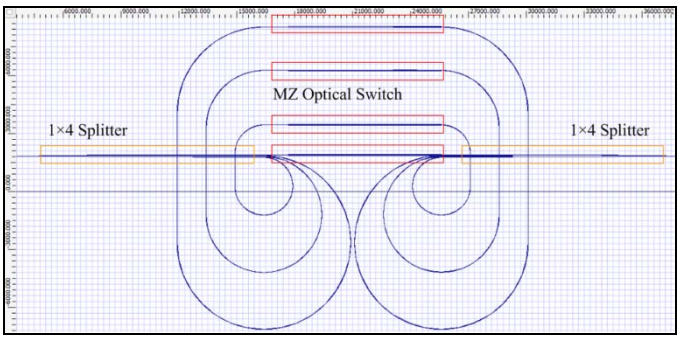

b

Fig. 1. Design of the OTTD devices: schematic of a 1×4 optical delay device (**a**) and schematic of a 2-bit optical delay device (**b**).

of the Y-branch is less than 1°. There are four paths in our design. Path 1 is a straight waveguide. The other paths are composed of a bend waveguide and straight waveguide. The bend radius of each path is fixed. The bend radii from inner to outer paths are 1.5, 3 and 4.5 mm. The lengths of straight connection waveguides from the inner to outer paths are 2.2, 4.4 and 6.6 mm (the corresponding length l is 2.2 mm in Fig. 1**a**). We made a design to introduce four MZ thermo-optic switches between two 1×4 OTTD elements to form a 2-bit optical delay device, as shown in Fig. 1**b**. The thermo-optic switch using SU-8 was reported before [22]. The integrated device which overcomes the topographical constraint can provide 0, 122, 244 and 366 ps time delays in a 1.5 cm×4 cm rectangular chip.

For OTTD device, the total insertion loss will be the sum of the coupling loss (including fiber to waveguide and waveguide to fiber) (I_{CL}), the input and output reflection losses (I_{RL}), the loss from the X junctions (I_{JL}), the bending loss (I_{BL}) from the waveguide delay lines, the mismatching losses (I_{ML}) between bend waveguides and straight waveguides and the total path propagation loss (I_{PL}). We demonstrated these losses separately below. The losses of each channel in a 1×4 OTTD are given as:

$$I_{loss1} = I_{CL} + 2I_{RL} + 3I_{JL} + I_{PL1} \tag{1}$$

$$I_{loss2} = I_{CL} + 2I_{RL} + 7I_{JL} + I_{BL2} + 4I_{ML} + I_{PL2} \tag{2}$$

$$I_{loss3} = I_{CL} + 2I_{RL} + 7I_{JL} + I_{BL3} + 4I_{ML} + I_{PL3} \tag{3}$$

$$I_{loss4} = I_{CL} + 2I_{RL} + 7I_{JL} + I_{BL4} + 4I_{ML} + I_{PL4} \tag{4}$$

Each of the channels 2, 3 and 4 has 4 connections of straight waveguide and bending waveguides. And the light passes through 7 X-junctions in the propagation in each channel. The bending loss is also introduced in these channels. So, the optical output power of the delay channel waveguide is attenuated gradually as the lengths increase.

2.1. Structure of waveguide

In order to reduce polarization sensitivity, the width and thickness of the waveguide core are selected to be equal. The dimension of the waveguide determines the quantity of modes in the waveguide and the coupling loss between the single mode fiber (SMF) and the waveguide. We simulate the coupling loss of the fiber to waveguide versus the waveguide dimension by beam propagation method (BPM). The coupling loss is shown in Fig. 2.

The core width and thickness are selected to be both 4 μm to keep single mode, and the coupling loss is 1.52 dB. The thickness of the upper cladding layer is important to the loss of the waveguide. We simulate the optical field distribution of the waveguide

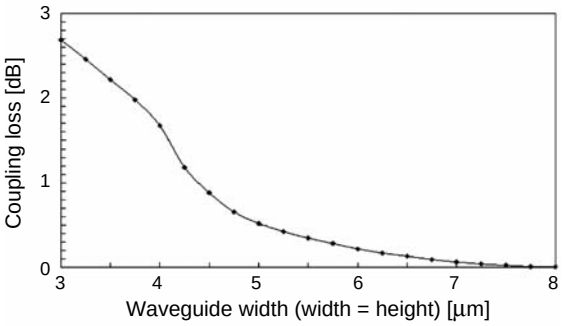

Fig. 2. Coupling loss vs. different waveguide dimensions.

profile by BPM. In order to decrease the loss of the waveguide, we should ensure that the waveguide dimension is larger than the optical field distribution region. So, the upper cladding layer thickness is selected to be 4 μm.

2.2. Right-angle X junction

Right-angle X-junction with two identical waveguides intersecting at 90° help overcome the topographical constraint in the design of long-length waveguide device within a confined area. The structure is shown in Fig. 3; n_{co} is the refractive index of the core, and n_{cl} is the refractive index of the cladding. The waveguide width is selected to be 2*a*.

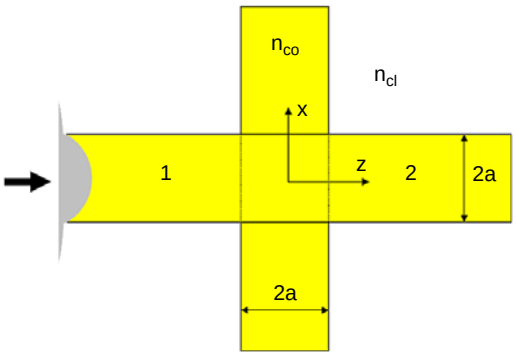

Fig. 3. The structure of the right-angle junction.

The transmission coefficient for the fraction of incident power leaving port 2 is found to be 99.8% in a 4×4 μm^2 waveguide using the beam propagation method (BPM) and a physical model reported before. The loss of the right junction is approximately 0.07 dB. When the angle is larger than 75°, the loss is below 0.13. The total loss of the X-junctions is 0.91 dB theoretically in the longest channel.

2.3. Bend waveguide

Curved waveguides are widely used in OTTD. The small radius bends are essential to achieve a higher packaging density of optical component in PICs to improve their

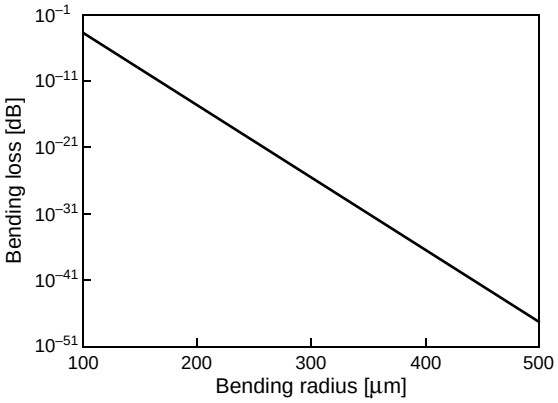

Fig. 4. Bending loss of the 4 μm×4 μm waveguide/90°.

Fig. 5. Device of S-bend composed of two 90° waveguides (**a**); near-infrared field of the device of S-bend (**b**).

functionality and reliability. The method of Marcuse is used to calculate pure bending loss. It can be seen from Fig. 4 that for R = 100 μm, the pure bending loss can be 0.1 dB per 90° turn. Comparing with the propagation loss, the bending loss is small enough when the bending radius is larger than 500 μm.

The bend loss is experimentally confirmed to be small. Different radius S-bend composed of two 90° circular waveguides were fabricated. Figure 5**a** shows schematic of the device. The radii from inner to outer paths were 500, 750, 1000, 1250, 1500 μm. We obtained a near-infrared field of the device in Fig. 5**b**, with 0.4 mW input power and in a 2 cm long sample. The losses were all below 10 dB. The result demonstrated that we can fabricate a device with the bend radius larger than 500 μm.

2.4. Propagation loss

Because of the low junction loss and low bend loss, the variation in insertion loss between adjacent paths is mainly caused by the different lengths of the waveguide. In the parameters given above, the propagation loss which is shown in Fig. 6 has been

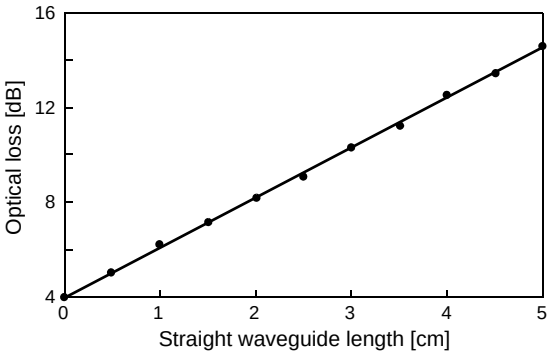

Fig. 6. Propagation loss of the waveguide with cladding.

calculated experimentally. Propagation loss of straight waveguide is 2 dB/cm. Though the propagation loss is a bit large, the material is cheap and easy to obtain. By using new highly fluorinated polymers, the propagation loss can be reduced to 0.07 dB/cm [23]. Then the total loss of the device can be dramatically reduced.

The fabrication process is listed below. An 8 μm thick film (NOA-61) was spin--coated (spin speed 4000 rpm, time ~20 s) on silicon substrate. The exposure was performed at 365-nm wavelength and 300-W Hg lamp power (100 mW/cm^2) for 7 min. A 4 μm thick core film was spin-coated on it (spin speed 3500 rpm, time ~20 s), prebaked at 60 °C for 10 min and at 90 °C for 20 min to remove any traces of solvent before exposure. The pattern exposure was performed at 365-nm wavelength and 350-mW Hg lamp power (10 mW/cm^2) for 3 min, then a post exposure baking was performed at 65 °C for 10 min and at 95 °C for 10 min to crosslink the polymer. The resist is developed in propyleneglygol monomethylether acetate (PGMEA) for 40 s, rinsed in isopropyl alcohol followed by deionised water, and blown dry to form the channel waveguides. After that, it is very important to cure the wafer by baking it at 150 °C for 30 min so that the adhesion between polymeric waveguide and the buffer layer can be well enhanced and the glass transition temperature T_g can be increased. To protect the waveguide and accidental scratches, it is necessary to

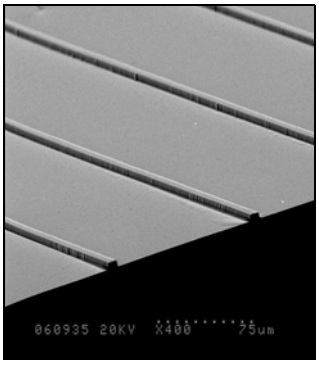

Fig. 7. The SEM of the SU-8 waveguide core.

spin-coat a 8 μm thick film (NOA-61) as upper cladding. The square waveguide sidewall roughness value scanned by the AFM was about 0.44 nm [24]. The SEM picture of the waveguide arrays is shown in Fig. 7.

The near-infrared field patterns of the 1×4 OTTD device are shown in Fig. 8. The optical output power of the delay channel waveguide is attenuated gradually as the lengths increase with the input power 2 mW. The extinction ratio of the MZ switch was –21 dB and the driving power was 10 mW. The switching property of the device was tested with DC bias. The rise time and the fall time of the switch were 0.9 ms and 0.6 ms. The loss of the switches is larger than that required in real-life systems, so they have not been integrated in the 2-bit OTTD system. To test the loss and time delay of the 2-bit OTTO device, a 1×4 OTTD element and a 4×4 OTTD element (the same structure without a 1×4 splitter) are integrated. A schematic photograph of the fabricated OTTD device is shown in Fig. 9. The insert losses of the 2-bit OTTD device are measured by the AQ8203 optical power meters. The total losses are 7.4, 15.11, 21.15, 27.74 dB.

Exact time delay values between adjacent channels were measured. A continuous--wave laser, operating at 1.55 μm, was modulated by a modulator fed by a network analyzer (HP37269C), which was used as the probe signal. The probe signal was input to the delay device. A photodetector covering the band frequency range was used to convert the modulated optical signal to an electrical signal that was fed back to the network analyzer.

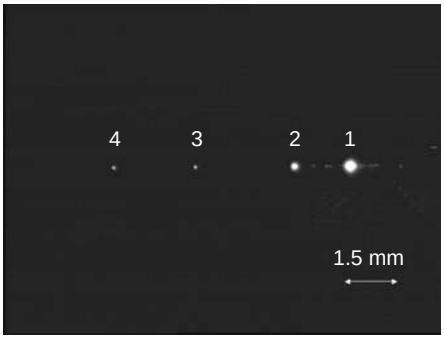

Fig. 8. Near-infrared field of the 1×4 OTTD.

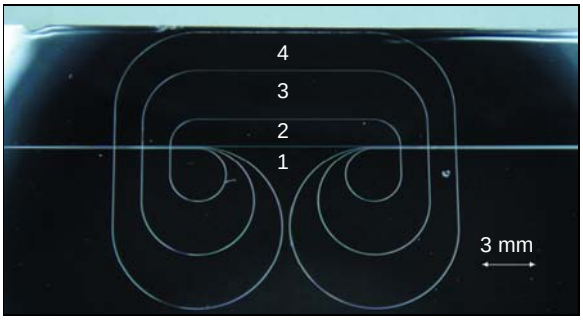

Fig. 9. Schematic photograph of 2-bit OTTD.

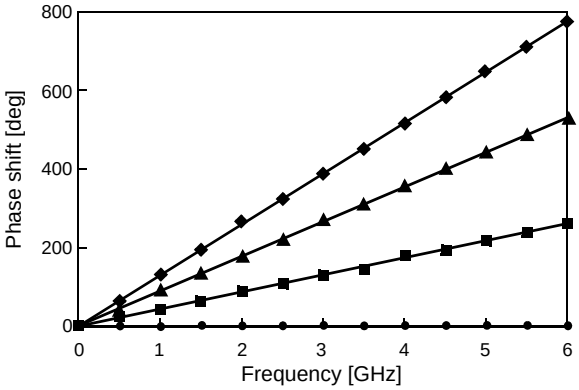

Fig. 10. Measurement results for each channel.

The delays between adjacent paths were given by the difference of each path. Figure 10 shows the measured microwave phase versus the frequency sampled from 0 to 6 GHz. The measured time delays of the 2-bit OTTD were 0, 121.1, 242.3, and 365.7 ps at 1550 nm. The experimental uncertainty in the delay measurement is 3 ps due to the jitter in the network analyzer's measurement of the phase.

3. Discussion and conclusions

A 2-bit true-time delay line using right-angle X junctions has been designed, fabricated and evaluated. This true-time delay line is compact, accurate, and easy to fabricate while providing a wide instantaneous bandwidth. The power consumption of the device is low. However, the insertion losses of the polymer delay device are currently larger than those required for actual PAA systems. These losses could be compensated by integrating with a polymer waveguide amplifier. Future work will include increasing the number of bits of the device while at the same time reducing the device size and insertion loss.

Acknowledgements – This work was supported by the National Natural Science Foundation of China (Nos. 61077041, 60807029), the Science Foundation for Young Scientists of Jilin Province, China (No. 20100174), Program for Special Funds of Basic Science and Technology of Jilin University (Nos. 200810028, 200905005) and the Opened Fund of State Key Laboratory on Integrated Optoelectronics (No. IOSKL-KFKT-11).

References

[1] GESELL L.H., FEINLEIB R.E., LAFUSE J.L., TURPIN T.M., *Acousto-optic control of time delays for array beam steering*, Proceedings of SPIE **2155**, 1994, pp. 194–204.

[2] MAAK P., FRIGYES I., JAKAB L., HABERMAYER I., GYUKICS M., RICHTER P., *Realization of true-time delay lines based on acoustooptics*, IEEE Journal of Lightwave Technology **20**(4), 2002, pp. 730–739.

[3] RIZA N.A., *Acousto-optic liquid-crystal analog beam former for phased-array antennas*, Applied Optics **33**(17), 1994, pp. 3712–3724.
[4] KOEPF G.A., *Optical processor for phased-array antenna beam formation*, Proceedings of SPIE **477**, 1984, pp. 75–81.
[5] ANDERSON L., BOLDISSAR F., KUNATH R., *Antenna beamforming using optical processor*, Antennas and Propagation Society International Symposium, Vol. 25, 1987, pp. 431–434.
[6] KONISHI Y., CHUJO W., FUJISE M., *Carrier-to-noise ratio and sidelobe level in a two-laser model optically controlled array antenna using Fourier optics*, IEEE Transactions on Antennas and Propagation **40**(12), 1992, pp. 1459–1465.
[7] RIZA N.A., *Liquid crystal-based optical time-delay control system for wideband phased arrays*, Proceedings of SPIE **1790**, 1993, p. 171.
[8] FETTERMAN H.R., CHANG Y., SCOTT D.C., FORREST S.R., ESPIAU F.M., WU M., PLANT D.V., KELLY J.R., MATHER A., STEIER W.H., OSGOOD R.M. JR., HAUS H.A., SIMONIS G.J., *Optically controlled phased array radar receiver using SLM switched real time delays*, IEEE Microwave and Guided Wave Letters **5**(11), 1995, pp. 414–416.
[9] YAO X.S., MALEKI L., *A novel 2-D programmable photonic time-delay device for millimeter--wave signal processing applications*, IEEE Photonics Technology Letters **6**(12), 1994, pp. 1463–1465.
[10] FRIGYES I., SEEDS A.J., *Optically generated true-time delay in phased array antennas*, IEEE Transactions on Microwave Theory and Techniques **43**(9), 1995, pp. 2378–2386.
[11] FU J., SCHAMSCHULA M., CAULFIELD H.J., *Modular solid optic time delay system*, Optics Communications **121**(1–3), 1995, pp. 8–12.
[12] DOLFI D., JOFFRE P., ANTOINE J., HUIGNARD J.-P., PHILIPPET D., GRANGER P., *Experimental demonstration of a phased-array antenna optically controlled with phase and time delays*, Applied Optics **35**(26), 1996, pp. 5293–5300.
[13] BOYD R.W., GAUTHIER D.J., GAETA A.L., WILLNER A.E., *Maximum time delay achievable on propagation through a slow-light medium*, Physical Review A **71**(2), 2005, article 023801.
[14] GUANSHI QIN, SOTOBAYASHI H., TSUCHIYA M., ATSUSHI MORI, SUZUKI T., OHISHI Y., *Stimulated Brillouin scattering in a single-mode tellurite fiber for amplification, lasing, and slow light generation*, IEEE Journal of Lightwave Technology **26**(5), 2008, pp. 492–498.
[15] YIHONG CHEN, XUPING ZHANG, RAY T. CHEN, *Substrate-guided-wave hologram-based continuously variable true-time-delay module for microwave phased-array antennas*, Proceedings of SPIE **4652**, 2002, p. 249.
[16] CHEN Y.H., CHEN R.T., *A fully packaged true time delay module for a K-band phased array antenna system demonstration*, IEEE Photonics Technology Letters **14**(8), 2002, pp. 1175–1177.
[17] CHEN Y.H., CHEN R.T., *K-band phased-array antenna system demonstration using substrate guided wave true-time delay*, Optical Engineering **42**(7), 2003, pp. 2000–2005.
[18] YEGNANARAYANAN S., TRINH P.D., COPPINGER F., JALALI B., *Compact silicon-based integrated optic time delays*, IEEE Photonics Technology Letters **9**(5), 1997, pp. 634–635.
[19] HOWLEY B., YIHONG CHEN, XIAOLONG WANG, QINGJUN ZHOU, ZHONG SHI, YONGQIANG JIANG, CHEN R.T., *2-bit reconfigurable true time delay line using 2×2 polymer waveguide switches*, IEEE Photonics Technology Letters **17**(9), 2005, pp. 1944–1946.
[20] HOWLEY B., WANG X.L., CHEN M., CHEN R.T., *Reconfigurable delay time polymer planar lightwave circuit for an X-band phased-array antenna demonstration*, IEEE Journal of Lightwave Technology **25**(3), 2007, pp. 883–890.
[21] CHANGMING CHEN, YUNJI YI, FEI WANG, YUNFEI YAN, XIAOQIANG SUN, DAMING ZHANG, *Ultra long compact optical polymeric array waveguide true-time-delay line devices*, IEEE Journal of Quantum Electronics **46**(5), 2010, pp. 754–761.

[22] LEI GAO, JIE SUN, XIAOQIANG SUN, CAIPING KANG, YUNFEI YAN, DAMING ZHANG, *Low switching power 2×2 thermo-optic switch using direct ultraviolet photolithography process*, Optics Communications **282**(20), 2009, pp. 4091–4094.

[23] YENIAY A., RENYUAN GAO, TAKAYAMA K., RENFENG GAO, GARITO A.F., *Ultra-low-loss polymer waveguides*, IEEE Journal of Lightwave Technology **22**(1), 2004, pp. 154–158.

[24] TUNG K.K., WONG W.H., PUN E.Y.B., *Polymeric optical waveguides using direct ultraviolet photolithography process*, Applied Physics A: Materials Science and Processing **80**(3), 2005, pp. 621–626.

Received April 12, 2011
in revised form July 18, 2011